CellPress

Cell Stem Cell
Article

NANOG and CDX2 Pattern Distinct Subtypes of Human Mesoderm during Exit from Pluripotency

Sasha Mendjan,[1,2,*] Victoria L. Mascetti,[1,2] Daniel Ortmann,[1,2] Mariaestela Ortiz,[1,2] Dyah W. Karjosukarso,[1,2] Yifan Ng,[1,2] Thomas Moreau,[1,2] and Roger A. Pedersen[1,2,*]

[1]The Anne McLaren Laboratory for Regenerative Medicine, Wellcome Trust-Medical Research Council Cambridge Stem Cell Institute, University of Cambridge, Cambridge CB2 0SZ, UK

[2]Department of Surgery, University of Cambridge, Cambridge CB2 0SZ, UK

*Correspondence: sm687@cam.ac.uk (S.M.), ralp2@cam.ac.uk (R.A.P.)

http://dx.doi.org/10.1016/j.stem.2014.06.006

SUMMARY

Mesoderm is induced at the primitive streak (PS) and patterns subsequently into mesodermal subtypes and organ precursors. It is unclear whether mesoderm induction generates a multipotent PS progenitor or several distinct ones with restricted subtype potentials. We induced mesoderm in human pluripotent stem cells with ACTIVIN and BMP or with GSK3-β inhibition. Both approaches induced BRACHYURY$^+$ mesoderm of distinct PS-like identities, which had differing patterning potential. ACTIVIN and BMP-induced mesoderm patterned into cardiac but not somitic subtypes. Conversely, PS precursors induced by GSK3-β inhibition did not generate lateral plate and cardiac mesoderm and favored instead somitic differentiation. The mechanism of these cell fate decisions involved mutual repression of NANOG and CDX2. Although NANOG was required for cardiac specification but blocked somitic subtypes, CDX2 was required for somitic mesoderm but blocked cardiac differentiation. In sum, rather than forming a common PS progenitor, separate induction mechanisms distinguish human mesoderm subtypes.

INTRODUCTION

Organ development in vertebrates begins with induction of the primary embryonic tissue layers ectoderm, mesoderm, and endoderm, and their subsequent patterning into specific tissue subtypes. The induction of mesoderm from pluripotent cells marks the onset of this process, evidenced by primitive streak (PS) formation (Arnold and Robertson, 2009; Stern et al., 2006; Tam and Loebel, 2007). The specification of mesoderm in the vertebrate embryo is initiated and driven by dynamic bone morphogenetic protein (BMP), NODAL/ACTIVIN, fibroblast growth factor (FGF), and WNT signaling gradients along the anterior-posterior axis of the embryo and the PS (Figure 1A). The same signaling activities are also essential for subsequent spatial and temporal allocation (or patterning) of mesodermal subtypes after PS induction. Fate-mapping experiments in vertebrates show that mesoderm patterning into subtypes strictly correlates with the place and time of mesoderm induction in the PS (Lawson et al., 1991; Tam et al., 1997). For instance, anterior-specific subtypes include anterior lateral plate and cardiac mesoderm, whereas extraembryonic and somitic mesoderm is exclusively posterior. However, it remains unclear how mesoderm induction and its patterning into organ precursors depend on diverse and changing signals during initial differentiation.

Mesoderm and its subtypes can be generated in vitro from human pluripotent stem cells (hPSCs), which provide a model of early human development and a major source of therapeutically relevant cell types (Murry and Keller, 2008; Nishikawa et al., 2007). Mesoderm can be induced from hPSCs by a remarkably wide range of conditions, including different signals that are present during PS formation (Kattman et al., 2011; Mae et al., 2013). Regardless of induction method, a common feature is expression of the early pan-mesodermal marker gene *BRACHYURY* (*BRA*) (Martin and Kimelman, 2010). However, there is no comprehensive human mesoderm induction and patterning model to test how different *BRA* and mesoderm induction signals direct efficient generation of distinct mesodermal subtypes and tissues.

At present, the dominant view is that different signaling environments during PS induction lead to a BRA$^+$ multipotent and unrestricted mesoderm progenitor that can be further specified into all mesodermal subtypes (Figure 1B). In an alternative model, different PS mesoderm induction signals could generate restricted BRA$^+$ mesoderm progenitors with differing potential to form distinct mesodermal subtypes. These two hypotheses lead to different and testable expectations regarding (1) different mechanisms of *BRA* induction, (2) distinct molecular identities of induced BRA$^+$ mesoderm, and (3) the dependency of mesoderm subtype specification on the initial PS induction mechanism. Finally, we hypothesized that if direction into distinct mesodermal subtypes depended on PS mesoderm induction, this could involve mutually exclusive exit mechanisms from pluripotency.

We tested these hypotheses by inducing PS mesoderm in hPSCs using FGF signaling in combination with ACTIVIN and BMP or with glycogen synthase kinase 3 β (GSK3-β) inhibition followed by subsequent specification into different mesodermal subtypes. First, we determined how these signaling pathways independently activated *BRA* expression. We then demonstrated that these different mechanisms of *BRA* and PS

mesoderm induction lead to distinct mesodermal subtypes. Finally, we showed that ACTIVIN/BMP and GSK3-β mediated these effects via NANOG and CDX2, respectively. Accordingly, our findings provide valuable insights into lineage specification mechanisms of therapeutically relevant tissues and organs.

RESULTS

Human PSCs can be differentiated into anterior PS-like (AnteriorPS) cells by combining phosphatidylinositol 3-kinase inhibition (using LY294002 [Ly]) with FGF2 (F), ACTIVIN A (A), and BMP4 (B), whereas Ly plus F and B induce posterior PS-like (PosteriorPS) cells (Bernardo et al., 2011; McLean et al., 2007). Subsequent differentiation leads to functional tissue derivatives of these PS regions (Figure S1A available online) (Cheung et al., 2012; Cho et al., 2012; Loh et al., 2014; Touboul et al., 2010). In addition to these signals, canonical WNT-driven, GSK3-β-mediated β-CATENIN signaling is a key pathway in mesoderm induction both in vivo and in vitro (Arnold and Robertson, 2009; Murry and Keller, 2008). WNT ligands lead, among other effects, to inhibition of GSK3-β activity causing stabilization of nuclear β-CATENIN, which acts as a potent transcriptional coactivator (Nusse and Varmus, 2012). To mimic these signals, we combined WNT agonists (recombinant WNT3A) or the GSK3-β inhibitor CHIR99021 (Ch) with AnteriorPS and PosteriorPS treatments in order to model vertebrate PS induction. Despite general advantages of small molecules like Ch in driving pluripotent stem cell (PSC) differentiation, we bore in mind that GSK3-β is not an exclusive mediator of WNT or β-CATENIN signaling and that it mimics only one of several WNT pathway branches. We then used F, A, B, and Ch separately and in combination to distinguish between direct patterning into subtypes by PS mesoderm induction versus patterning after PS induction of a multipotent mesoderm precursor (Figure 1B).

ACTIVIN/BMP Signaling and GSK3-β Inhibition Can Both Induce Mesoderm

Unlike NODAL and BMP, which form anterior-posterior signaling gradients in the early vertebrate PS, FGF and WNT signaling is active throughout the PS at all stages (Aulehla and Pourquié, 2010). Accordingly, we inhibited GSK3-β using Ch in combination with either F alone or AnteriorPS or PosteriorPS conditions. Cells induced to differentiate with Ch showed a distinctive, cobblestoned morphology and strong upregulation of pan-PS markers BRA and *TBX6* compared to PosteriorPS and AnteriorPS treatments (Figures S1C, 1C, 1E, and S1D). We confirmed this in live hPSCs carrying a fluorescent reporter of endogenous *BRA* transcription involving a histone 2B (H2B)-Venus fusion knockin (Figure 1D). We observed higher levels, more homogeneous population intensity peaks, and widespread activation of *BRA* expression with Ch (Figures 1C and 1D). An immunoflow analysis of BRA protein suggests more transient dynamics of BRA up- and downregulation with AnteriorPS treatment as compared to F plus Ch (Figure S1D). In conclusion, whereas GSK3-β inhibition strongly induced BRA and *TBX6*, ACTIVIN and BMP signaling induced them only moderately. However, it remained unclear whether these different PS induction mechanisms were similar or distinct.

Because GSK3-β inhibition can markedly boost BRA expression, we asked whether it could do this independently of exogenous FGF, ACTIVIN, or BMP signaling. Exogenous F and Ch were sufficient to induce the *BRA*-VENUS-H2B reporter, *BRA* transcription, and protein expression (Figures 1C, 1F, and S1D). Moreover, when we blocked ACTIVIN (SB431542 [Sb], SIS3), BMP (Dorsomorphin), and FGF/ERK pathways (SU5402, PD0325901), we still observed significant induction of BRA transcript and protein expression by GSK3-β inhibition alone (Figures 1G, S1E, and S1F). By contrast, PosteriorPS and AnteriorPS induction of BRA expression depended entirely on ACTIVIN/BMP combined with FGF signaling (Figures 1C and S1E).

We then asked the reciprocal question whether WNT and GSK3-β signaling is essential for ACTIVIN/BMP-dependent BRA induction. WNT Luciferase reporter activity and upregulation of the WNT target *AXIN2* in PosteriorPS cells were initially very low (after 18 hr) and increased only later (after 36 hr) compared to conditions containing WNT agonists (WNT3A, R-Spondin, or Ch). This is in agreement with the identification of WNT3/WNT3A as targets of BRA (Figures 1H and 1I) (Evans et al., 2012; Martin and Kimelman, 2008). Furthermore, inhibition of WNT signaling in PosteriorPS cells (using DKK1 or IWR1) did not diminish induction of BRA or the mesoderm marker *MESP1*, which is consistent with the modest nuclear localization of β-CATENIN in PosteriorPS cells (Figures S1H, 1J, and S1G). These results indicated that PosteriorPS induced BRA expression in the presence of low endogenous canonical WNT signaling. We concluded that ACTIVIN/BMP signaling and GSK3-β inhibition could act in parallel to induce expression of pan-mesodermal marker genes.

ACTIVIN/BMP and GSK3-β Control *BRA* Expression via Distinct Transcriptional Regulatory Elements

To clarify how diverse mesoderm induction mechanisms intersect at the *BRA* locus, we performed chromatin immunoprecipitation (ChIP) followed by quantitative PCR (qPCR) for chromatin binding components of the ACTIVIN (SMAD2/SMAD3), BMP (SMAD1/SMAD5), and canonical WNT (β-CATENIN) pathways in pluripotency, AnteriorPS, and AnteriorPS plus Ch conditions. We observed SMAD2/SMAD3 and SMAD1/SMAD5 binding to two putative regulatory regions (proximal and distal; Figures 2A, S2A, and 2C) upstream of *BRA* in both differentiation conditions. SMAD2/SMAD3 bound both proximally and distally, but SMAD1/SMAD5 bound predominantly distally in a region with known DNase hypersensitivity and a putative enhancer (Figure S2A; Loh et al., 2014). By contrast, β-CATENIN bound mainly in the AnteriorPS plus Ch condition to the proximal promoter region. SMAD2/SMAD3 bound mostly to the proximal promoter region in pluripotent conditions. Luciferase assay analysis further confirmed that only a long 6 kb fragment containing the distal SMAD1/SMAD5 site could drive *BRA* expression in PosteriorPS condition (Figure 2B). By contrast, a short 1 kb fragment containing the proximal promoter was sufficient to strongly stimulate *BRA* expression by the PosteriorPS plus Ch condition. We concluded that induction of *BRA* is mediated by distinct transcriptional regulatory elements. Taken together, these results demonstrate how a limited set of signals can induce *BRA*

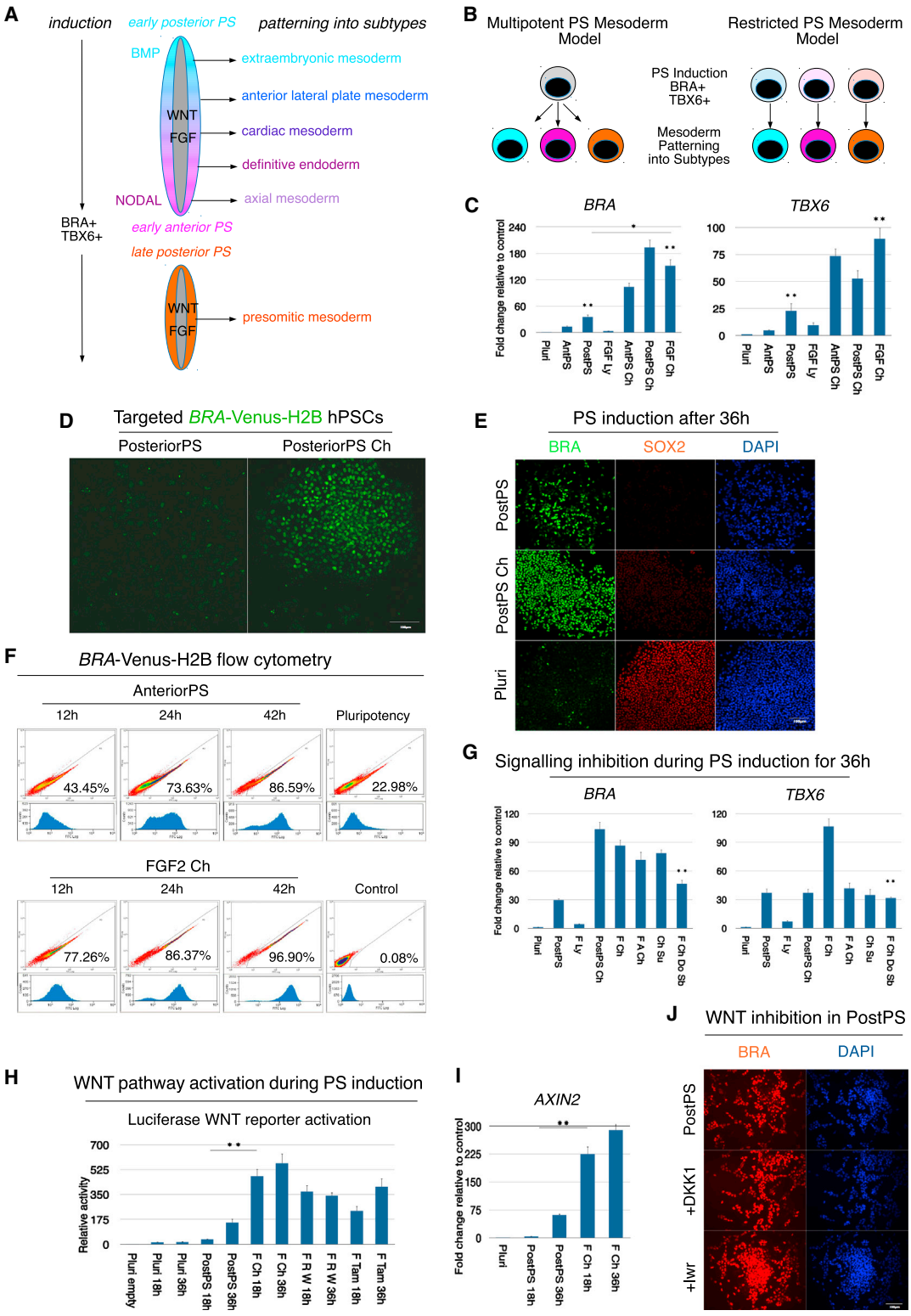

Figure 1. ACTIVIN/BMP Signaling and GSK3-β Inhibition Can Both Induce Mesoderm

(A) Simplified scheme of mesoderm induction and patterning defined by signaling gradients (BMP high in posterior; NODAL/ACTIVIN high in anterior) and activities (FGF and WNT high in streak) in distinct regions of the PS at different stages.

(B) Two hypothetical models of mesoderm induction and patterning.

(legend continued on next page)

and mesoderm differentiation by distinct mechanisms that have sufficient complexity to generate potentially different mesoderm subtypes.

ACTIVIN/BMP Signaling or GSK3-β Inhibition Induces Distinct AnteriorPS, PosteriorPS, and LatePS Mesodermal Identities

In contrast to BRA and TBX6, which are expressed throughout PS development, other early mesodermal markers show more localized expression in either the anterior or the posterior of the early PS or in the late PS at the onset of somitogenesis (Aulehla and Pourquié, 2010; Tam and Loebel, 2007). We therefore asked whether other key mesodermal markers were coexpressed with BRA in either ACTIVIN/BMP-dependent treatments or in conditions with GSK3-β inhibition, using RT-qPCR, immunocytochemistry, and immunoflow analysis. As previously shown, PosteriorPS cells induced early PS, extraembryonic, and lateral plate mesoderm transcripts (*CDX2*, *HAND1*, *KDR*, and *MESP1*), whereas AnteriorPS cells induced mid and anterior PS markers (*EOMES* and *GSC*; Figures 3A, 3C, and 3E; Bernardo et al., 2011). By contrast, AnteriorPS plus Ch and PosteriorPS plus Ch treatments both induced exclusively markers of late PS and presomitic mesoderm (MSGN1, TBX6, CDX1, CDX2, and *CDX4*; Figures 3A, 3B, S3B, and S3C). Because F plus Ch alone also activated all of these late PS mesoderm markers, we regarded this condition as inducing late PS-like (LatePS) differentiation (Figures 3A, 3C, and 3D). Furthermore, we found that CDX2 expression levels, similar to BRA, depended on Ch dosage (3 versus 8 μM) and that both markers strongly colocalized (Figure S3A). These results echoed vertebrate embryo gastrulation, where a gradient of strong, posterior WNT and FGF signaling induces high levels of BRA, TBX6, and CDX proteins in the late PS mesoderm (Aulehla and Pourquié, 2010; Lohnes, 2003). Importantly, the identification of distinct BRA^+ PS mesoderm progenitors (AnteriorPS versus PosteriorPS versus LatePS; Figure 3D) allowed us to test whether they are multipotent or restricted in their subsequent subtype specification potential. The strengths of this in vitro model thus enabled a rigorous analysis of the mechanism whereby cells exit pluripotency and become specified into mesodermal subtypes.

AnteriorPS Induction, but Not PosteriorPS Induction, Patterns hPSCs into Cardiac Mesoderm

We previously used PosteriorPS induction to subsequently pattern hPSCs into lateral plate mesoderm (with F plus B) and to differentiate further into functional smooth muscle cells (SMCs) (Bernardo et al., 2011; Cheung et al., 2012). We now used this approach to ask whether PosteriorPS induction could give rise to other lateral plate derivatives such as cardiac mesoderm and beating cardiomyocytes.

In vivo studies implicate retinoic acid (RA) and inhibition of canonical WNT signaling in mesoderm patterning into the cardiac lineage (Marvin et al., 2001; Niederreither et al., 2001). Consistent with this, we combined RA and IWR1 (AXIN stabilizer inhibiting canonical WNT signaling) during lateral plate treatment and boosted expression of cardiac markers NKX2-5, *TBX5*, *MYH6*, and *MYL7* after 5 days of differentiation (Figures 4A and S4A). However, further differentiation did not result in beating cardiomyocytes, and cardiac structural marker expression decreased (data not shown). If mesoderm induction affects later mesoderm patterning, PosteriorPS induction might not support formation of some mesoderm subtypes, including cardiac. Alternatively, the multipotent mesoderm precursor hypothesis predicts that all PS treatments should generate cardiac progenitors and beating cardiomyocytes.

We examined these possibilities using different PS treatments followed by a 6-day chemically defined, 2D cardiac differentiation protocol involving F plus B together with RA and IWR1. Strikingly, whereas AnteriorPS treatment induced robust formation of beating clusters, PosteriorPS or PosteriorPS plus Sb induction followed by identical treatment did not result in cardiac differentiation (Figure 4B). Functional cardiomyocyte differentiation was achieved at a wide range of A concentrations (20–100 ng/ml) but most effectively at intermediate levels (50 ng/ml; Figures 4C and S5A). This method was successfully employed with different human embryonic stem cell (hESC) lines and with induced hPSCs (HES3, H7, H9, and BOB; Figures 4C and S4B). When generated at lower initial seeding densities, we could quantify functional beating clusters, whereas higher seeding densities resulted in cluster networks or beating cardiomyocyte sheets (Movie S1). AnteriorPS-induced cells upregulated cardiac structural markers MYL7, TROPO-T, and α-ACTININ as well as endogenous *NKX2-5*, as shown using the GFP reporter gene knockin HES3 hPSC line (Figure 4C). By contrast, PosteriorPS or PosteriorPS plus Sb treatments did not activate or maintain high expression of key cardiac transcription factors NKX2-5, ISL1, HAND1, and GATA6 (Figures S4C and S4D). Our results suggest that the prerequisite for efficient cardiac specification occurs in the first 36 hr of mesoderm induction. These results do not support the hypothesis

(C) RT-qPCR analysis of transcript levels for the general PS markers *BRA* and *TBX6* in H9 hESCs grown in pluripotency conditions (Pluri; FGF plus ACTIVIN) or F (FGF) plus Ly AnteriorPS (AntPS; FGF plus ACTIVIN plus BMP plus Ly), PosteriorPS (PostPS; FGF plus BMP plus Ly), or with FGF plus the GSK3-β inhibitor Ch. Further details are in Experimental Procedures.

(D) Confocal images of live H9 hESCs with *Venus-H2B* reporter targeted to the endogenous *BRA* locus.

(E) Confocal images of H9 hESCs (Pluri) or after 36 hr in PosteriorPS conditions.

(F) Flow cytometry of H9 hESCs showing *BRA* levels and expression dynamics in AnteriorPS and FGF plus Ch conditions.

(G) GSK3-β inhibition independently induces *BRA* and *TBX6*. RT-qPCR analysis of transcript levels of *BRA* and *TBX6* with indicated combinations of Ch and F, A, B, Dorsomorphin (Do), SU5402 (Su), or SB431542 (Sb) is shown.

(H) Luciferase WNT activity reporter assay in stably transfected ΔN-β-CATENIN-ER-inducible H9 hESCs after 18 and 36 hr of differentiation induced by FGF (F) with WNT3A (W), R-SPONDIN-1 (R), or 4-hydroxy-tamoxifen (Tam).

(I) RT-qPCR expression analysis of the canonical WNT signaling target gene *AXIN2* in indicated conditions.

(J) PosteriorPS conditions induce BRA independently of canonical WNT signaling, as shown by treatment with the WNT receptor inhibitor DKK-1 or the AXIN stabilizer IWR1 (Iwr).

*$p < 0.05$, **$p < 0.005$, versus Pluri or pairwise as indicated by bar. Scale bars, 100 μM.

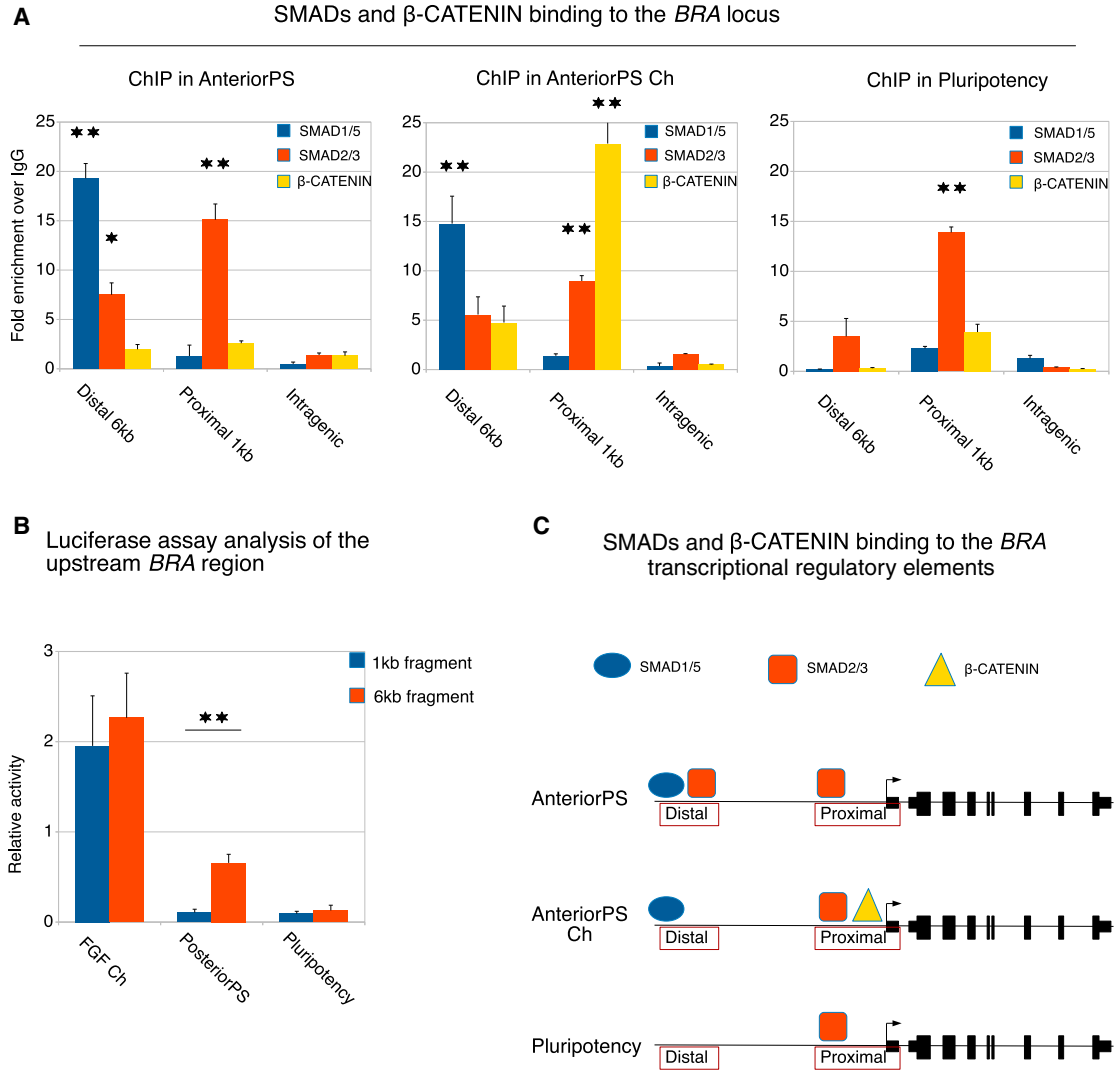

Figure 2. ACTIVIN/BMP Signaling and GSK3-β Inhibition Control *BRA* Expression via Distinct Transcriptional Regulatory Elements

(A) ChIP-qPCR analysis of SMADs and β-CATENIN binding performed using primers as shown in Figure S2A.

(B) Luciferase reporter analysis of transiently transfected H9 hESCs with indicated fragments (A).

(C) Model of SMAD1/5, SMAD2/3, and β-CATENIN binding.

*$p < 0.05$, **$p < 0.005$, versus control or pairwise as indicated by bar.

of a multipotent mesoderm PS precursor, which predicted equivalent capabilities for cardiomyocyte development following PosteriorPS or AnteriorPS induction. They favor instead the alternative hypothesis of early mesodermal subtype patterning via PS precursors of restricted differentiation potential.

GSK3-β Inhibition during AnteriorPS Induction Blocks Cardiac Specification

Although A and B were both required during AnteriorPS induction for efficient cardiac differentiation, the roles of WNT signaling and GSK3-β inhibition were unclear at this stage. Modest GSK3-β inhibition by Ch (3 μM) or inhibition of upstream WNT signaling (both canonical and noncanonical) by IWP2 during AnteriorPS induction prevented specification into beating, α-ACTININ$^+$ cardiomyocyte clusters (Figure 4D). Consistent with this, Ch and IWP2 treatment during induction inhibited the upregulation of the lateral plate mesoderm markers *MESP1*, NKX2-5, ISL1, GATA6, and HAND1 after lateral plate and cardiac differentiation (Figures 4F, S4F, and S4E). This inhibitory effect of Ch during PS induction was not due to nuclear β-CATENIN because Tam-induced translocation of stably transfected ΔN-β-CATENIN-ER did not block NKX2-5 upregulation (Figures S4F, 1H, and 6D). Moreover, Ch did not inhibit cardiac differentiation when it was added after the initial induction step (Figure S4G). In contrast to Ch or IWP2, inhibition of canonical WNT signaling by AXIN stabilizers IWR1 or XAV939 during AnteriorPS induction did not affect cardiac differentiation (Figure 4D). We therefore hypothesized and confirmed that additional, noncanonical WNT-JNK signaling is required during cardiogenic AnteriorPS induction (Figures 4D and 4E). Taken

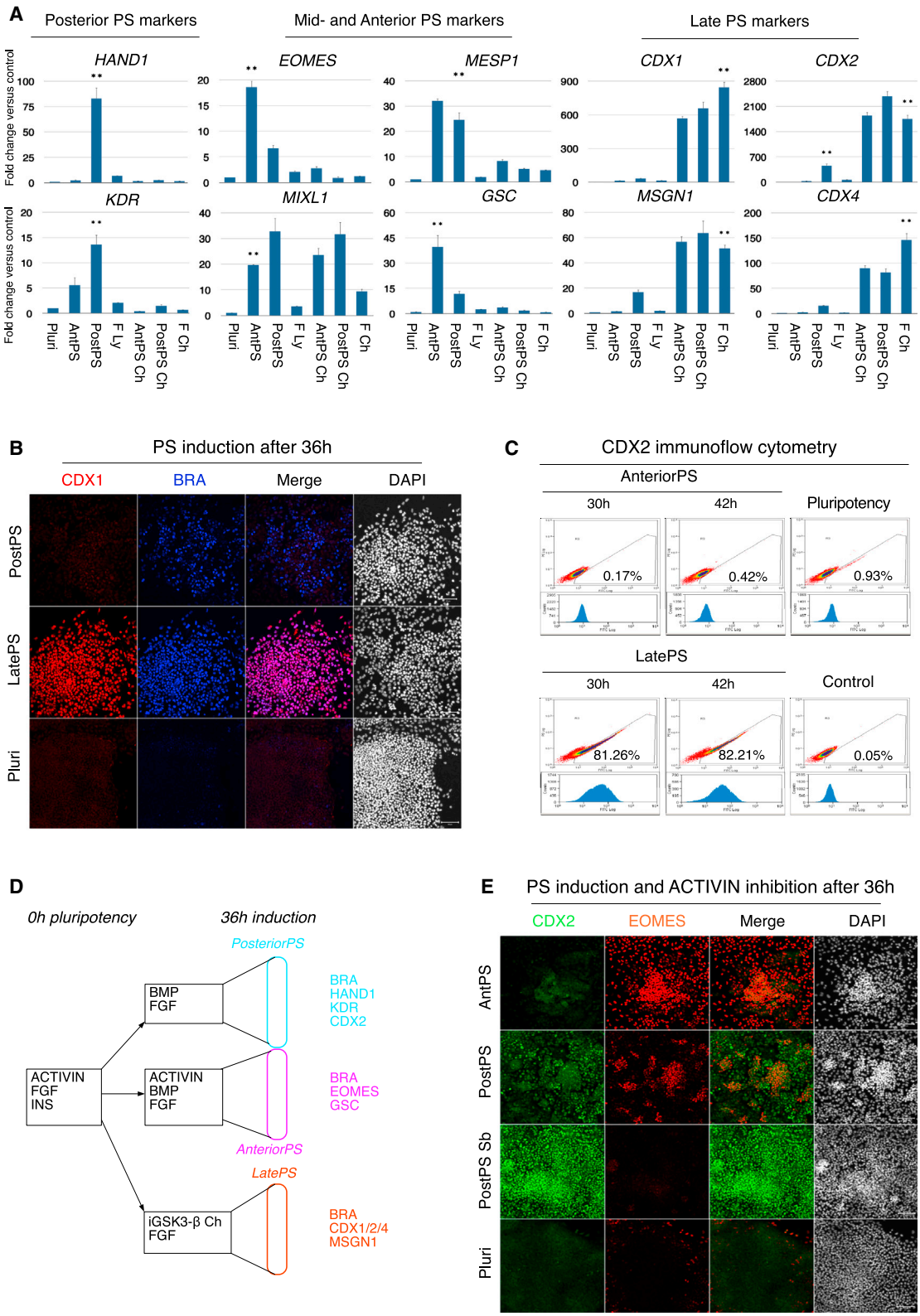

Figure 3. ACTIVIN/BMP Signaling or GSK3-β Inhibition Induces Distinct PosteriorPS, AnteriorPS, and LatePS Mesodermal Identities

(A) RT-qPCR analysis of indicated early mesodermal transcripts in H9 hESCs grown in mesoderm-inducing conditions.

(B) F plus inhibition of GSK3-β (LatePS) induces the late PS marker CDX1, which colocalizes with BRA and is not upregulated by PosteriorPS treatment. Representative confocal images of H9 hESCs are shown.

(legend continued on next page)

together, these observations further support the hypothesis that early PS induction is critical for later patterning of mesoderm into lateral plate and cardiac subtypes.

Cardiac mesoderm and definitive endoderm (DE) share the requirement for the anterior PS marker EOMES, which has been shown to activate the precardiac determinant MESP1 (Costello et al., 2011). We found that inhibition of GSK3-β or inhibition of ACTIVIN signaling blocked *MESP1* and EOMES upregulation during AnteriorPS induction (Figures 3A, 4F, and 4G). In agreement with this, hPSCs in DE plus Ch condition did not upregulate DE markers EOMES, SOX17, and FOXA2, suggesting that strong GSK3-β inhibition also prevented DE differentiation (Figures 4G, S4H, and S4I). These effects were independent of nuclear β-CATENIN and depended instead on Ch dosage and exogenous F and B (Figures S4K, 4G, 4D, and S4J). In summary, derivatives of the early mid and anterior PS: DE, lateral plate, and cardiac mesoderm are blocked by strong inhibition of GSK3-β or inhibition of ACTIVIN signaling during PS induction. These signals lead instead to the upregulation of CDX2, a marker and determinant of posterior extraembryonic mesoderm and the late PS (Figure S4L; Lohnes, 2003).

LatePS and PosteriorPS Cells Are Committed and Cannot Undergo Patterning into Cardiac Lineage

DE is known to have an inductive role in cardiac specification in vivo and in vitro (Mummery et al., 2007; Schultheiss et al., 1995). A possible explanation for the negative effect of GSK3-β inhibition on cardiac differentiation is that cardiogenic inductive signals from FOXA2$^+$ AnteriorPS or DE cells are absent (Figures 5A and S5A). We therefore tested whether GFP-labeled LatePS cells could differentiate efficiently into cardiac lineage when they were mixed with nonlabeled AnteriorPS cells during cardiac differentiation. Interestingly, GFP-labeled LatePS-induced cells could not generate beating cardiac clusters even in the presence of AnteriorPS-derived nonlabeled cells, suggesting that they are already committed to other fates (Figure 5B). Similarly, GFP-labeled PosteriorPS cells mixed with unlabeled AnteriorPS cells did not generate beating clusters (data not shown). This result does not contradict the established role of DE during later cardiac specification but argues against a dominant instructive role during AnteriorPS induction. Accordingly, we hypothesized that PosteriorPS and LatePS conditions cannot generate cardiac mesoderm because they induce early lineage determinants that drive commitment to other mesodermal subtypes.

LatePS Induction Promotes Patterning into (Pre)Somitic Mesoderm in Contrast to PosteriorPS and AnteriorPS Induction

According to our models in Figures 3D and S4L, LatePS treatment was sufficient to induce presomitic mesoderm markers that are expressed in the posterior region of the embryo after formation of DE, lateral plate, and cardiac mesoderm. The hypothesis that mesoderm subtype patterning depends on PS induction predicts that further patterning treatments on LatePS cells would generate (pre)somitic (presomitic and somitic) mesoderm precursors of muscle and cartilage instead of lateral plate or cardiac mesoderm. We treated LatePS cells with RA and a lower dose of F thereby mimicking conditions during (pre)somitic mesoderm differentiation in the vertebrate embryo (Aulehla and Pourquié, 2010). We observed the upregulation of (pre)somitic markers (*TCF15*, *MESP2*, *MEOX1*, MYF5, *PAX1*, *ZO-1*, SOX9, and PAX3); conversely, the PS marker TBX6 was efficiently downregulated (Figures 5C, 5D, 5H, S5B, and S5C). Interestingly, upregulation of PAX3 (together with PAX7, the key determinants of the skeletal muscle lineage) and SOX9 (early sclerotome/chondrogenic determinant) was completely blocked by B in LatePS and by PosteriorPS or AnteriorPS induction (Figures 5D and 5E). Importantly, when we treated cells after (pre)somitic differentiation with F plus B as we did during cardiac differentiation, we observed specific upregulation of chondrogenic (cartilage) markers *COL2A1* and *ACAN* instead of cardiac markers (Figure S5E). To confirm that LatePS-derived (pre)somitic cells differentiated into chondrogenic, extracellular matrix-producing cells, we used Alcian blue and found widespread proteoglycan staining (Figure 5F). Moreover, PosteriorPS or AnteriorPS induction with identical subsequent treatments resulted in inefficient chondrogenic differentiation, confirming that GSK3-β inhibition used in LatePS condition is crucial for subsequent somite-like mesoderm specification. In conclusion, whereas PosteriorPS and AnteriorPS induction promotes subsequent patterning into lateral plate and cardiac mesoderm, LatePS conditions instead promote patterning into (pre)somitic fates (model in Figure 5G).

SMCs Can Be Generated after AnteriorPS, PosteriorPS, and LatePS Mesoderm Induction

We asked next whether patterning of all mesoderm cell types depends on early PS induction. SMCs are a particularly interesting case because these are generated at all stages and from all segments of the PS and could be therefore less sensitive to PS mesoderm induction conditions (Majesky, 2007). Accordingly, we induced PS mesoderm with AnteriorPS, PosteriorPS, and LatePS conditions and then applied an identical lateral plate patterning treatment (F plus B) followed by functional SMC differentiation (platelet-derived growth factor BB [PDGF-BB] plus transforming growth factor β [TGF-β]; Figures 5I and S5D). These SMCs showed clear morphological differences suggesting that they were separate populations with distinct developmental origins as seen before (Figure S5F; Cheung et al., 2012). After 9 days of SMC differentiation, all three induction treatments resulted in the expression of key SMC markers (CNN1, ACTA2, *MYH11*, and *TAGLN*; Figures 5I and S5D) in the absence of other mesodermal markers (NKX2.5, PAX3, and BRA; data not shown). Upregulation of these markers was blocked by (pre)somitic patterning treatment (F plus RA; Figure 5I). Importantly, upon treatment with Carbachol (which induces SMC contractions), SMCs derived from all PS treatments showed contractile activity,

(C) Time course immunoflow cytometry quantification of CDX2$^+$ cells in AnteriorPS and LatePS conditions.
(D) Hypothesized human in vitro PS induction model.
(E) Representative confocal images of PS treatments, showing mutually exclusive CDX2 and EOMES expression.
**$p < 0.005$, versus Pluri. Scale bars, 100 μM.

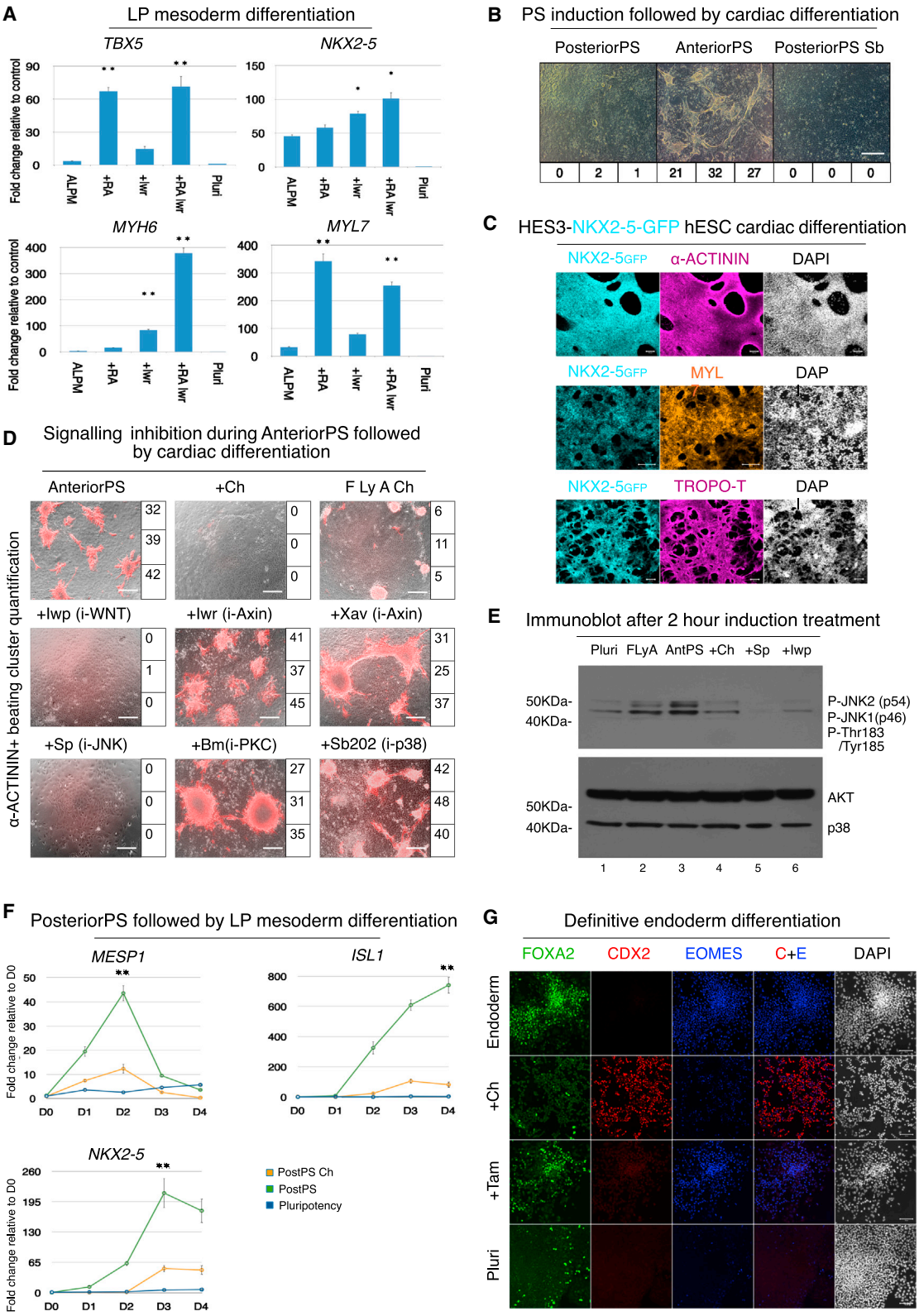

Figure 4. AnteriorPS Induction Is Required for Cardiac Specification

(A) RA treatment and inhibition of canonical WNT signaling by IWR1 (Iwr) promote the expression of cardiac transcription factors *TBX5* and *NKX2-5* as well as cardiomyocyte structural proteins *MYL7* and *MYH6* during lateral plate mesoderm (LPM; F+B, 4 days) differentiation in H9 hESCs (see protocol in Figure S4L).

(legend continued on next page)

thereby confirming their functional capabilities, whereas control PosteriorPS-derived extraembryonic cells did not (Figures 5J, S5F, and S5G). Taken together, these findings support the hypothesis that mesoderm subtype specification begins with PS induction, and they argue against a multipotent mesoderm progenitor. This effect is particularly clear with mesodermal subtypes that emerge at a defined time and place during PS formation. We therefore explored the molecular basis of these cell fate decisions and examined determinants capable of directing mesodermal patterning at the earliest stages of PS exit from pluripotency and ensuing differentiation.

PosteriorPS, AnteriorPS, and LatePS Pattern Mesoderm via NANOG and CDX2

Two linked processes occur during AnteriorPS-, PosteriorPS-, and LatePS-induced differentiation: dynamic downregulation of so-called pluripotency factors (e.g., *OCT4*, *SOX2*, and *NANOG*); and the upregulation of early lineage determinants (e.g., *BRA*, *EOMES*, and *CDX2*). At first, we focused on *NANOG* because its expression differed most extensively between the distinct mesoderm induction conditions we employed here. Although NANOG expression was rapidly downregulated within 24 hr of GSK3-β inhibition and by reduced or blocked ACTIVIN signaling, it persisted in AnteriorPS cells (Figures 6A and 6B). NANOG protein colocalized with EOMES and was coexpressed with *MESP1* during the first 24–48 hr in AnteriorPS condition (Figures 6C and S6A). Notably, in AnteriorPS plus Ch induction, cells with high EOMES were distinct from those with high CDX2 protein levels (only 1.4% signal overlap; Figure S4I). Conversely, CDX2 expression was strongly upregulated in conditions where ACTIVIN signaling and NANOG expression were absent and either inhibition of GSK3-β or B was present (Figure 6A). The inhibitory effect of Ch on NANOG and EOMES expression in AnteriorPS condition could be reversed by IWR1 treatment. This coincided with partial β-CATENIN relocation to the cytoplasm and downregulation of CDX2 (Figures S6B and S6C). In contrast to induction of BRA, transcriptional activation by inducible nuclear β-CATENIN was not sufficient to downregulate NANOG or to upregulate CDX2, suggesting alternative regulation (Figure 6D). However, activation of CDX2 expression was still absolutely dependent on Ch (Figure S6D). These observations strongly implicate additional mediators of GSK3-β signaling as being involved in mesoderm induction and patterning. We concluded that PosteriorPS, AnteriorPS, and LatePS induction differed not only by differentiation marker expression but also in the exit mechanism from pluripotency.

NANOG Is Required for AnteriorPS-Induced Mesodermal Patterning, and CDX1/CDX2 Are Required for LatePS-Induced Mesodermal Patterning

A role for NANOG in mesoderm and endoderm differentiation has been proposed before by Loh and Lim (2011), but not in the context of mesoderm subtype specification via PS induction. We therefore explored the requirement of NANOG for mesoderm patterning by differentiating hPSCs stably expressing small hairpin RNAs (shRNA) directed against NANOG (NANOG knockdown [KD]). NANOG-KD clones could be passaged normally, and they expressed similar levels of SOX2 and OCT4 as control cells; they showed moderately activated CDX1/CDX2 but not TBX6 expression in pluripotency and AnteriorPS conditions (Figure S6E). Strikingly, depletion of NANOG caused a total absence of beating structures and reduced the expression of TROPO-T during cardiac differentiation, but not that of the lateral plate and extraembryonic mesoderm marker HAND1 (Figure 6E). NANOG-KD clones could differentiate into somitic mesoderm, chondrocytes, or SMCs, as seen by expression of PAX3 and SOX9, Alcian staining analysis, and ACTA2 and CNN1, respectively (Figures 6E and 6F; data not shown). Taken together, these results show that NANOG is required for the differentiation of AnteriorPS-derived cardiac mesoderm, but not for LatePS-derived somitic mesoderm or for ubiquitously derived mesodermal cell types, such as SMCs.

The requirement for NANOG in anterior (cardiac) mesoderm differentiation is complementary to the essential role of BRA and CDX factors in posterior (somitic and extraembryonic) mesoderm development (van Rooijen et al., 2012). Accordingly, we tested whether *CDX1/CDX2* (which are highly redundant)-KD clones differentiated into either cardiac or somitic lineages. Although *CDX1/CDX2*-KD clones upregulated NKX2.5 during cardiac differentiation and formed beating structures similar to the control, they failed to upregulate PAX3 and SOX9 during somitic differentiation and did not stain for Alcian blue after chondrogenic treatment (Figures 6F and 6G). Furthermore, *CDX1/CDX2*-KD clones had a proliferation defect and underwent increased apoptosis in LatePS and extraembryonic mesoderm differentiation (data not shown). These results confirmed that *CDX1/CDX2* play a similarly essential role during LatePS-induced differentiation as NANOG plays during AnteriorPS-induced differentiation.

Reciprocal Inhibition of NANOG and CDX2 Directs Patterning into Mesodermal Subtypes

The requirement of NANOG for anterior PS-derived and requirement of *CDX1/CDX2* for posterior PS-derived mesoderm led us

(B) Indicated PS induction treatments followed by cardiac differentiation as in (A) and another 48 hr in F plus B. ACTIVIN signaling in PosteriorPS condition was inhibited by Sb. Beating clusters were counted in triplicate after 8 days of differentiation (shown below each panel).
(C) Beating cardiomyocytes express major cardiac structural proteins in targeted *NKX2-5-GFP* HES3 hESCs. Representative confocal images are stained as indicated.
(D) Inhibition of upstream WNT signaling by IWP2 (Iwp), of GSK3-β by Ch and of JNK by SP600125 during AnteriorPS condition blocks cardiogenic differentiation in H9 hESCs. AXIN stabilization by IWR1 (Iwr) or XAV939 (Xav), PKC inhibition by Bisindolylmaleimide II (Bm), and p38 inhibition by SB202190 (Sb202) had no effect. α-ACTININ$^+$ beating clusters were counted as in (B) (right side of each panel).
(E) Phosphorylation of JNK1/JNK2 is reduced by noncardiogenic treatments during PS induction.
(F) GSK3-β inhibition blocks expression of lateral plate mesoderm markers in H9 hESCs induced by PosteriorPS condition (day 1 [D1}/D2) and followed by F plus B (D3/D4).
(G) Representative confocal images of a ΔN-β-CATENIN-ER-inducible H9 hESC clone after 48 hr of DE differentiation with addition of Ch or 4-hydroxy-tamoxifen (Tam).
*$p < 0.05$; **$p > 0.005$ versus LPM or D0. Scale bars, 100 μM.

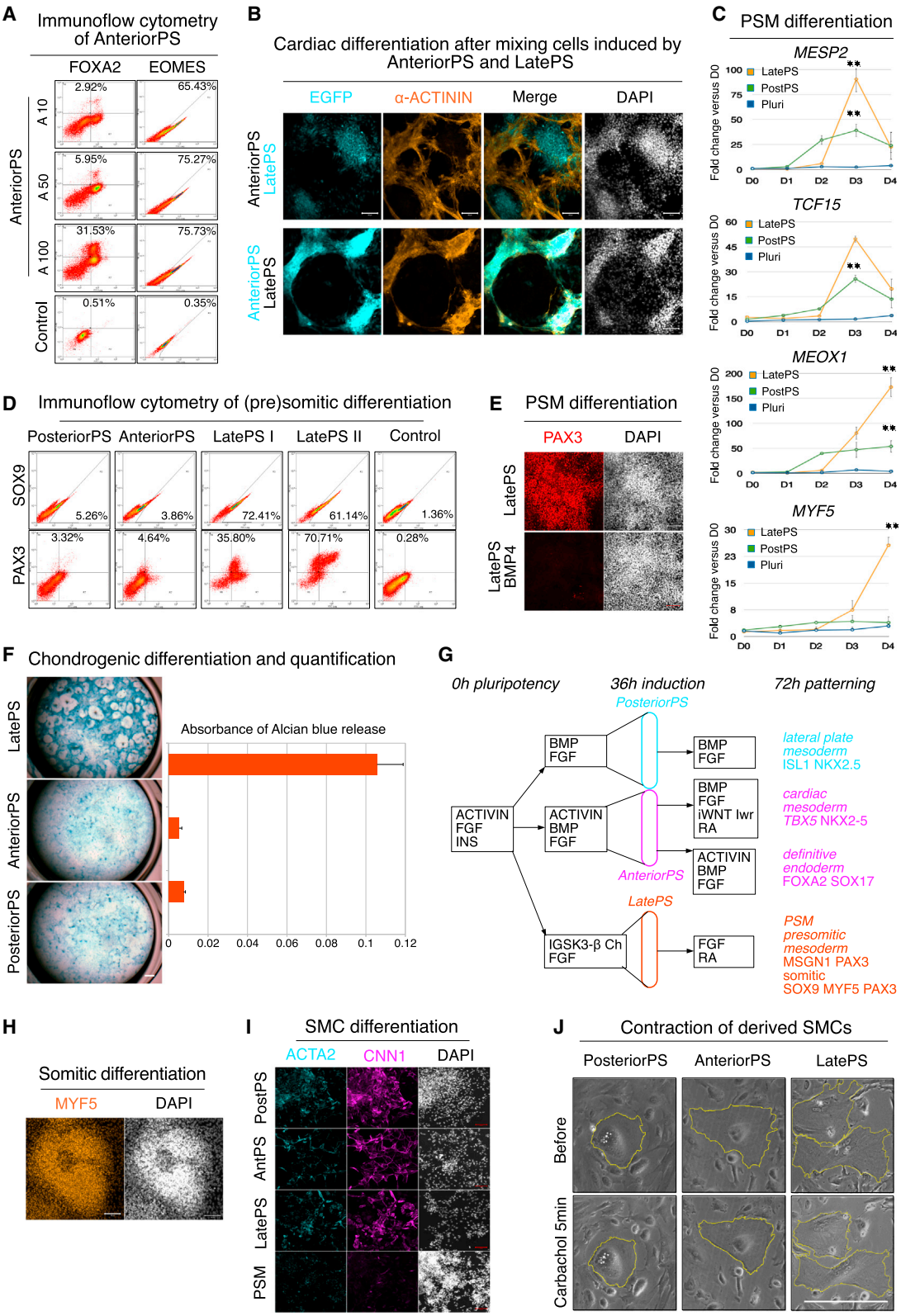

Figure 5. LatePS Induction Promotes Subsequent (Pre)Somitic Mesoderm Specification in Contrast to PosteriorPS and AnteriorPS Induction

(A) Immunoflow cytometry analysis of FOXA2$^+$ (top gated areas) and EOMES$^+$ (lower right-gated areas) cells induced by AnteriorPS condition with 10, 50, and 100 ng/ml ACTIVIN. Percentages of positive cells are indicated.

(legend continued on next page)

to ask whether NANOG and CDX2 were sufficient to act as determinants of these lineages. We overexpressed NANOG in hPSCs (NANOG-OE) and placed the resulting clones into AnteriorPS, PosteriorPS, and LatePS conditions. NANOG-OE clones differentiated normally in AnteriorPS but not in PosteriorPS and LatePS conditions (showing increased apoptosis). CDX2 upregulation was blocked depending on ACTIVIN signaling (Figures 7A and S7A; data not shown). Conversely, when we transduced hPSCs with a lentiviral vector expressing CDX2 to similar levels as in LatePS, we observed that CDX2 strongly repressed NANOG but not SOX2 expression (Figure 7B). CDX2 overexpression was mutually exclusive of high EOMES and high SOX17 expression at the onset and during AnteriorPS-induced DE differentiation (Figures S7B and S7C). Furthermore, BRA was highly induced in CDX2-transduced cells in conditions with ACTIVIN signaling (Figure S7B). This suggests a mutual positive regulation of CDX2 and BRA, with both acting as key determinants of posterior mesoderm development (Bernardo et al., 2011; Savory et al., 2009). Taken together, these results demonstrate a negative regulatory interaction between NANOG (which acts as an early specifier of anterior mesoderm and DE) and CDX2 (which acts as a specifier of posterior mesoderm). Importantly, this negative interaction loop between NANOG and CDX2 provided a mechanistic explanation and support for the hypothesis of mesodermal subtype patterning by PS induction.

Finally, we explored in detail how ACTIVIN and GSK3-β signaling gradually establish the observed reciprocal inhibition between NANOG and CDX2 in pluripotency and at the onset of AnteriorPS and LatePS induction. First, we performed a ChIP-qPCR analysis in AnteriorPS- and LatePS-treated cells using antibodies against SMAD2/SMAD3, NANOG, β-CATENIN, CDX2, and the transcriptional repressor TCF7L1 (ortholog of mouse TCF3). We chose TCF7L1 because it is essential for mesoderm development, it is a mediator of GSK3-β signaling that is highly expressed in hPSCs, and it is a putative target of NANOG and ACTIVIN signaling (Figure S7E; Brown et al., 2011; Merrill et al., 2004). NANOG, SMAD2/SMAD3, and in particular TCF7L1 bound putative regulatory regions (UCSC/ENCODE; Loh et al., 2014) in intron 1 of *CDX1* and *CDX2* in pluripotency and in AnteriorPS-treated cells (Figures 7D, S7D, and 7F). Moreover, TCF7L1 bound to a distal putative regulatory region of *NANOG* in LatePS-treated cells after 2 hr but not after 12 hr of treatment, which is consistent with rapid NANOG downregulation (Figures 7E and S7E). Unlike TCF7L1, β-CATENIN remained bound at the *CDX1* and *CDX2* intron 1 after 12 hr of induction. Once induced, CDX2 bound close to a distal putative regulatory region of *NANOG* exclusively in LatePS-treated cells (Figure 7C). These results are consistent with reports on the direct regulation of CDX genes by canonical WNT signaling (Lohnes, 2003). However, much less is known about how this pathway might regulate NANOG expression and thereby directs mesoderm patterning by the exit mechanism from pluripotency.

To resolve this question, we sought functional evidence for the observed transcription factor binding patterns at the *NANOG* locus. We used a Luciferase reporter assay to perform a detailed time course analysis of different *NANOG* transcriptional regulatory regions in AnteriorPS- and LatePS-treated cells. Interestingly, a 2.2 kb fragment upstream of *NANOG* containing several putative TCF binding sites inhibited reporter expression after 12 hr but not after 36 hr in LatePS condition (Figure 7G). In contrast, a short fragment of the NANOG promoter containing only previously characterized SMAD2/SMAD3 binding sites was not able to mediate any repression by GSK3-β inhibition during LatePS treatment. This argues against the possibility that GSK3-β inhibition impacts on NANOG expression by interfering with SMAD2/SMAD3 signaling. Instead, these results are consistent with the model that GSK3-β signaling inhibits NANOG expression via TCF7L1, which can also interfere with β-CATENIN binding and function (Wu et al., 2012). In further support of this hypothesis, transcriptional activation by inducible nuclear Δ-N-β-CATENIN could activate CDX2 only in the absence of NANOG and TCF7L1 when ACTIVIN signaling was inhibited (Figure S7F). This result finally explained why induced Δ-N-β-CATENIN alone did not recapitulate the negative effects of GSK3-β inhibition on cardiac and endoderm differentiation because these are most likely mediated by TCF7L1 and its repression of *NANOG*. In conclusion, surprisingly early events during mesoderm induction in hPSCs have dramatic consequences for mesoderm patterning. The interplay between ACTIVIN/BMP and GSK3-β signaling during PS induction thereby culminates in the reciprocal repression of NANOG and CDX2, enabling direct mesoderm specification into anterior and posterior subtypes.

DISCUSSION

We have used hPSCs as an experimental model to determine whether and how PS induction affects subsequent mesoderm patterning. We found evidence that BRA transcription and PS mesoderm can be induced independently by either ACTIVIN/

(B) EGFP-overexpressing H9 hESCs were induced by either AnteriorPS or LatePS condition then mixed and subjected to cardiac differentiation. Representative confocal images are shown.
(C) LatePS condition promotes differentiation of cells expressing markers of (pre)somitic (*MESP2*, *TCF15*) and somitic (*MEOX1*, *MYF5*) mesoderm. Daily transcript levels in H9 hESCs induced by 2-day PS treatments followed by 2-day treatment in F plus RA are shown.
(D) Immunoflow cytometry analysis of $SOX9^+$ and $PAX3^+$ cells induced by indicated treatments. LatePS I corresponds to presomitic differentiation after 72 hr. LatePS II corresponds to somitic differentiation after 4.5 days.
(E) B treatment during LatePS induction prevents upregulation of PAX3 in presomitic (PSM) differentiation.
(F) Chondrocytes emerge from somitic treatment followed by 10 days of F plus B. Proteoglycan production was quantified by Alcian blue staining and release.
(G) Hypothesized human in vitro PS induction and patterning model.
(H) Prolonged differentiation in CDM after somitic differentiation treatment maintains expression of MYF5. Representative confocal images of H9 hESCs after 7 days of differentiation are shown.
(I) SMCs resulting from PS induction followed by lateral plate or (pre)somitic treatments and PDGF plus TGF-β differentiation for 10 days. Representative confocal images of SMC markers ACTA2 and CNN2.
(J) Carbachol-induced contraction of SMCs derived from different PS inductions.
**$p > 0.005$ versus D0. Scale bars, 100 μM.

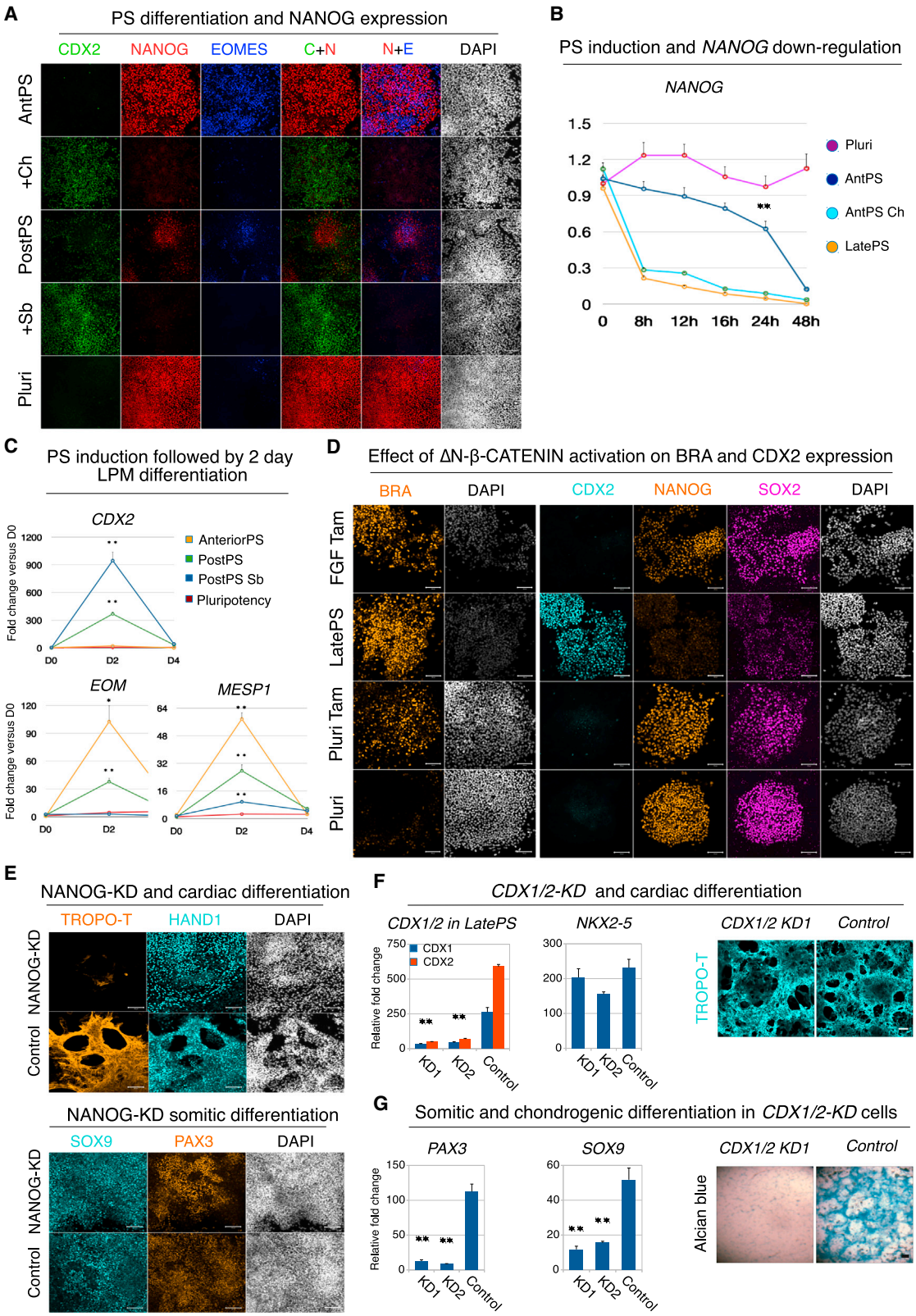

Figure 6. PosteriorPS, AnteriorPS, and LatePS Pattern Mesoderm via NANOG and CDX Factors

(A) GSK3-β inhibition by Ch and ACTIVIN signaling inhibition by Sb repress NANOG and upregulate CDX2. Representative confocal images of H9 hESCs treated and stained as indicated are shown.

(legend continued on next page)

BMP signaling or GSK3-β inhibition, which are, as in other vertebrates, mediated by distinct *BRA* transcriptional regulatory elements (Harvey et al., 2010). Our results indicate that these different mechanisms of PS induction produce cells of distinct identities (PosteriorPS, AnteriorPS, and LatePS) that presage mesoderm patterning into either lateral plate and cardiac or (pre)somitic subtypes. However, not all mesodermal cell types were restricted in their potential by PS induction, as seen with differentiation of SMCs, which are generated throughout gastrulation from all segments of the PS (and from neural crest). It will be important to determine whether SMCs derived by these separate mesoderm induction methods differ in their susceptibility to injury or disease (Cheung et al., 2012; Majesky, 2007). In contrast to SMCs, cardiac and (pre)somitic mesoderm emerge at a more defined time and place during gastrulation, which might explain their strong reliance on PS induction conditions. Finally, by exploring the mechanistic basis of these observations, we demonstrated that mesoderm patterning is defined by different exit mechanisms from pluripotency that depend on NANOG downregulation dynamics and its mutual repression by CDX2.

Based on insights gained here, together with knowledge of vertebrate gastrulation, we propose a working model and gene regulatory network of human PS mesoderm induction and patterning (Figure 7H). At the outset of PS induction, burgeoning FGF and BMP signals overcome NODAL/ACTIVIN signaling in the early posterior PS causing rapid downregulation of NANOG and upregulation of BRA and of CDX2 (major determinant of extraembryonic mesoderm). In the early anterior PS, increased NODAL/ACTIVIN signaling, together with FGF and BMP, induces EOMES and MESP1. Sustained by NOADAL/ACTIVIN signaling, NANOG, together with SMAD2/SMAD3 and its target TCF7L1, represses CDX factors that would otherwise block lateral plate, cardiac, and DE differentiation. In the late PS, FGF and strong GSK3-β inhibition (with low NODAL/ACTIVIN and BMP signaling) represses *NANOG* expression by stimulation of the TCF7L1 repressor. As NANOG and its putative target TCF7L1 become downregulated, β-CATENIN is able to induce high levels of BRA and CDX factors, which enables late PS-derived (pre)somitic mesoderm specification. Finally, we propose that reciprocal inhibition between NANOG and CDX2 similar to that previously described for the trophoblast and inner cell mass lineages (Chen et al., 2009) is harnessed during mesoderm development and patterning.

This model does not depict how moderate differences in signaling dosage might lead to even subtler distinctions between related PS derivatives. Moreover, the precise mechanistic role of factors like SMAD2/SMAD3 and TCF7L1 in pluripotency compared to PS induction needs to be addressed. Nevertheless, our results are consistent with the recent careful revaluation of murine *Wnt3* mutants that can initiate gastrulation and with the compound *Brachyury* and *Cdx2* knockout phenotypes in mouse embryos where posterior but not anterior mesoderm and DE are compromised (van Rooijen et al., 2012; Savory et al., 2009; Tortelote et al., 2013). Our findings revise the current concept of the role of NANOG in pluripotency and mesoderm differentiation to one that is more consistent with its in vivo expression and function during early PS- but not late PS-derived mesoderm development (Osorno et al., 2012).

There are significant conceptual implications of these insights into human mesoderm and general tissue induction and patterning. We suggest that what is collectively called PS mesoderm is instead a collection of specified mesodermal tissues with distinct identities and plasticities. In the mouse embryo, mesoderm formation begins at embryonic day 6.25 and continues until the PS disappears almost 3 days later. In humans, this period is extended further to a week during which the embryo undergoes dramatic changes in size, morphogenesis, tissue composition, and signaling. Accordingly, it should not be surprising that distinct subtypes of mesoderm emerge from hPSC differentiation depending on exposure to different BMP, ACTIVIN, FGF, and GSK3-β-mediated conditions. However, embryonic mesoderm might be more plastic and prone to compensation mechanisms, and careful in vivo studies should be used to test the model presented here.

There are also important practical implications of this study for hPSC differentiation into mesoderm and its derivatives. Most significantly, mesodermal cell types that have been difficult to generate may be produced more efficiently by initiating their differentiation through correct PS mesoderm induction and patterning. Although recent progress in the differentiation of some mesodermal lineages affirms this assessment (Kennedy et al., 2012; Mae et al., 2013; Xu et al., 2013), the current study provides the mechanistic underpinning and comprehensive explanations for it. Not only will this insight have a high impact on directed differentiation approaches from hPSCs but also it is likely to affect approaches like transcription factor-mediated reprogramming, which depends on starting cell and (germ layer) tissue subtype (Ladewig et al., 2013). Moreover, our observations might extend to neural and nonneural ectoderm induction and subtype patterning. Like mesodermal development, ectoderm patterning is directed by signaling gradients, and in vitro differentiation into distinct neural subtypes also shows variable efficiencies. Our insight that different PS mesoderm induction methods define human mesoderm subtype specification in hPSCs is therefore likely to have a major impact on the accessibility of key tissues for regenerative medicine.

(B) GSK3-β inhibition strongly represses *NANOG* expression during the first 24 hr of AnteriorPS and Late PS induction. Time course RT-qPCR analysis in H9 hESCs treated as indicated is shown.
(C) Inhibition of ACTIVIN signaling by Sb in PosteriorPS condition upregulates *CDX2* and inhibits *EOMES* and *MESP1*. Treatment protocol and transcript levels in H9 hESCs undergoing LP mesoderm differentiation are shown.
(D) Tamoxifen-inducible activation of ΔN-β-CATENIN-ER is sufficient to induce BRA but not CDX2 expression. H9 hESCs were induced and stained as indicated and examined by confocal microscopy.
(E) shRNA-mediated KD of NANOG abolishes cardiomyocyte (TROPO-T$^+$) differentiation but not somitic (SOX9$^+$, PAX3$^+$) differentiation. Cells were immunostained as indicated and examined by confocal microscopy.
(F) shRNA-mediated KDs (KD1 and KD2) of *CDX1*/*CDX2* do not affect *NKX2-5* and TROPO-T expression during cardiac differentiation but (G) repress *PAX3* and *SOX9* upregulation after somitic treatment and prevent Alcian blue-positive chondrocyte differentiation.
*$p < 0.05$; **$p > 0.005$ versus 0 hr, D0, or Control, respectively. Scale bars, 100 μM.

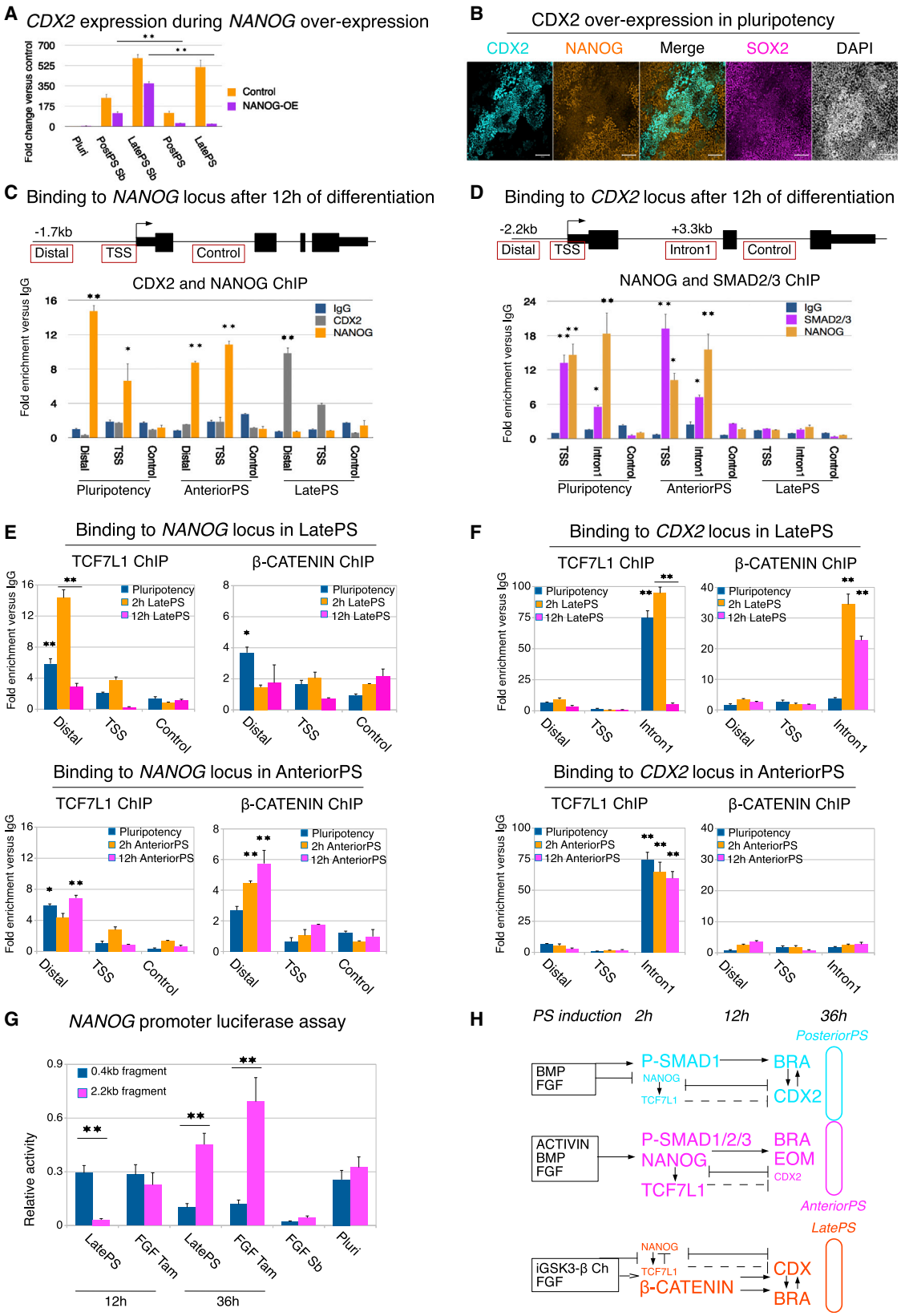

(legend on next page)

EXPERIMENTAL PROCEDURES

hPSC Differentiation into PS Mesoderm and Derivatives

hESCs (H9, H7, and HES3-NKX2-5-GFP) and induced PSCs (iPSCs) (BOB) were grown in chemically defined medium (CDM) with A (10 ng/ml) and F (12 ng/ml) and as described in the Supplemental Experimental Procedures. All differentiations were performed in CDM. PosteriorPS condition was induced by F (20 ng/ml), Ly (10 μM; Sigma-Aldrich), and B (10 ng/ml; R&D Systems) typically for 36 hr. AnteriorPS condition was induced as PosteriorPS plus A at either 50 ng/ml for cardiac or 100 ng/ml for DE differentiation. Full DE differentiation required 3 days. LatePS condition was induced by F (20 ng/ml) and Ch (8 μM; Tocris) in CDM without insulin. Lateral plate mesoderm treatment consisted of F (8 ng/ml) and B (10 ng/ml) for 2 or 4 days in CDM following PS induction. (Pre)somitic mesoderm was initiated after LatePS induction by F (4 ng/ml) and RA (1 μM; Sigma-Aldrich) for 36 hr and 4 days for somitic differentiation. Extraembryonic differentiation was initiated by B (20 ng/ml) for 3 days following PosteriorPS induction. SMC differentiation was initiated by TGF-β1 (2 ng/ml) and PDGF-BB (10 ng/ml) following PS induction and 4 days of lateral mesoderm treatment.

Chemically Defined 2D Cardiac Differentiation

One day after passaging, cardiogenic differentiation was initiated after AnteriorPS induction (with 50 ng/ml of A) by 4 days in F (8 ng/ml), B (10 ng/ml), IWR1 (1 μM; Tocris), and RA (1 μM; Sigma-Aldrich) followed by 2 days in CDM with F plus B. Cells were afterwards maintained in CDM. Onset of beating was observed on day 7 or 8 of differentiation in clusters (low initial colony density) or sheets (high initial colony density). The method was also routinely performed on hESC lines H7 and HES3 as well as in several human iPSC lines.

Chondrogenic Differentiation and Alcian Blue Staining

Chondrocyte differentiation was initiated after LatePS induction and 4 days of somitic treatment (F plus RA) by F (8 ng/ml) and B (10 ng/ml) in CDM for 10 days. For Alcian blue staining, cells were fixed in 4% paraformaldehyde, washed with PBS, and stained in 0.025% Alcian solution (pH 2.0).

Flow Cytometry

For quantitative analysis of *BRA*-Venus-H2B reporter gene activity and intracellular transcription factor staining, cells were grown in different conditions and then dissociated into single cells using Cell Dissociation Buffer (Gibco). Cells were washed with PBS, where appropriate, stained as described previously (BD Biosciences; Bernardo et al., 2011), and run on a CyAn ADP flow cytometer (Beckman Coulter).

ChIP

ChIP was carried out as described previously by Brown et al. (2011) with the modification that pluripotent and differentiated hESCs were fixed in Hank's balanced salt solution (pH 7.6) containing 1% formaldehyde and protein crosslinkers disodium phosphate and tryptose phosphate broth (Sigma-Aldrich) for 20 min at room temperature. Antibodies and primers are described in the Supplemental Experimental Procedures. Results were expressed as relative pull-down amount when normalized against the immunoglobulin G control ChIP for the same region, and fold change was calculated. Relative enrichments were then compared to a control region. Data are representative of three experiments performed on the same day, and error bars indicate SD.

Statistical Analysis

Statistical significance of quantitative data was determined by applying a two-tailed Student's test to raw values or to the average values obtained from independent experiments. Detailed Experimental Procedures and information about used reagents can be found in the Supplemental Experimental Procedures.

SUPPLEMENTAL INFORMATION

Supplemental Information for this article includes Supplemental Experimental Procedures, seven figures, and one movie and can be found with this article online at http://dx.doi.org/10.1016/j.stem.2014.06.006.

AUTHOR CONTRIBUTIONS

S.M. designed, conducted, and analyzed the experiments and wrote the paper. D.O. and V.L.M. contributed as equal second authors by conducting and analyzing some of the experiments and by generating reagents. M.O. and T.M. generated reagents. D.W.K. and Y.N. conducted some of the experiments. R.A.P. supervised the study and wrote the paper.

ACKNOWLEDGMENTS

We thank Tiago Faial, Paulina Latos, and Kathy Niakan for helpful comments. We are grateful to Stefania Carobbio and Antonio Vidal-Puig for help and support. We thank Stephanie Brown, Alessandro Bertero, Ludovic Vallier, H. Suemori, Jane Bardwell, Andrew Elefanty, Edward Stanley, Barry Rosen, and Bill Skarnes (Wellcome Trust Sanger Institute, EUCOMMTOOLs program) for expert advice, collaboration, and key reagents. This work was supported by EMBO (postdoctoral fellowship to S.M.), British Heart Foundation PhD fellowships (to D.O. and V.L.M.), UK Medical Research Council and British Heart Foundation grants (to R.A.P.), and the Cambridge Hospitals National Institute for Health Research Biomedical Research Centre funding (to R.A.P.). R.A.P. is a cofounder of DefiniGEN, a UK start-up company that generates hepatocytes and other endodermal cell types for drug development and toxicity testing. This work was done, however, entirely independently of DefiniGEN.

Received: September 19, 2013
Revised: April 23, 2014
Accepted: June 6, 2014
Published: July 17, 2014

REFERENCES

Arnold, S.J., and Robertson, E.J. (2009). Making a commitment: cell lineage allocation and axis patterning in the early mouse embryo. Nat. Rev. Mol. Cell Biol. *10*, 91–103.

Aulehla, A., and Pourquié, O. (2010). Signaling gradients during paraxial mesoderm development. Cold Spring Harb. Perspect. Biol. *2*, a000869.

Bernardo, A.S., Faial, T., Gardner, L., Niakan, K.K., Ortmann, D., Senner, C.E., Callery, E.M., Trotter, M.W., Hemberger, M., Smith, J.C., et al. (2011). BRACHYURY and CDX2 mediate BMP-induced differentiation of human and mouse pluripotent stem cells into embryonic and extraembryonic lineages. Cell Stem Cell *9*, 144–155.

Figure 7. Reciprocal Inhibition of NANOG and CDX2 Directs Early Specification into Mesodermal Subtypes

(A) NANOG repression of *CDX2* depends on ACTIVIN signaling.
(B) Lentiviral CDX2 overexpression inhibits NANOG but not SOX2 expression in pluripotent conditions. Representative confocal images of transiently transfected H9 hESCs are shown.
(C) CDX2 and NANOG ChIP-qPCR at the *NANOG* locus.
(D) NANOG and SMAD2/SMAD3 ChIP-qPCR at the *CDX2* locus.
(E) TCF7L1 and β-CATENIN ChIP-qPCR binding analysis at the *NANOG* and (F) *CDX2* loci using indicated conditions and primer positions from (C) and (D).
(G) Luciferase reporter analysis of transiently transfected H9 hESCs with indicated fragments.
(H) Human in vitro PS induction model outlining the gene regulatory network that controls mesoderm patterning via different PS induction mechanisms.
*$p < 0.05$; **$p > 0.005$ versus control or pairwise as indicated with bar. Scale bars, 100 μM.

Brown, S., Teo, A., Pauklin, S., Hannan, N., Cho, C.H., Lim, B., Vardy, L., Dunn, N.R., Trotter, M., Pedersen, R., and Vallier, L. (2011). Activin/Nodal signaling controls divergent transcriptional networks in human embryonic stem cells and in endoderm progenitors. Stem Cells *29*, 1176–1185.

Chen, L., Yabuuchi, A., Eminli, S., Takeuchi, A., Lu, C.W., Hochedlinger, K., and Daley, G.Q. (2009). Cross-regulation of the Nanog and Cdx2 promoters. Cell Res. *19*, 1052–1061.

Cheung, C., Bernardo, A.S., Trotter, M.W., Pedersen, R.A., and Sinha, S. (2012). Generation of human vascular smooth muscle subtypes provides insight into embryological origin-dependent disease susceptibility. Nat. Biotechnol. *30*, 165–173.

Cho, C.H., Hannan, N.R., Docherty, F.M., Docherty, H.M., João Lima, M., Trotter, M.W., Docherty, K., and Vallier, L. (2012). Inhibition of activin/nodal signalling is necessary for pancreatic differentiation of human pluripotent stem cells. Diabetologia *55*, 3284–3295.

Costello, I., Pimeisl, I.-M., Dräger, S., Bikoff, E.K., Robertson, E.J., and Arnold, S.J. (2011). The T-box transcription factor Eomesodermin acts upstream of Mesp1 to specify cardiac mesoderm during mouse gastrulation. Nat. Cell Biol. *13*, 1084–1091.

Evans, A.L., Faial, T., Gilchrist, M.J., Down, T., Vallier, L., Pedersen, R.A., Wardle, F.C., and Smith, J.C. (2012). Genomic targets of Brachyury (T) in differentiating mouse embryonic stem cells. PLoS One *7*, e33346.

Harvey, S.A., Tümpel, S., Dubrulle, J., Schier, A.F., and Smith, J.C. (2010). no tail integrates two modes of mesoderm induction. Development *137*, 1127–1135.

Kattman, S.J., Witty, A.D., Gagliardi, M., Dubois, N.C., Niapour, M., Hotta, A., Ellis, J., and Keller, G. (2011). Stage-specific optimization of activin/nodal and BMP signaling promotes cardiac differentiation of mouse and human pluripotent stem cell lines. Cell Stem Cell *8*, 228–240.

Kennedy, M., Awong, G., Sturgeon, C.M., Ditadi, A., LaMotte-Mohs, R., Zúñiga-Pflücker, J.C., and Keller, G. (2012). T lymphocyte potential marks the emergence of definitive hematopoietic progenitors in human pluripotent stem cell differentiation cultures. Cell Reports *2*, 1722–1735.

Ladewig, J., Koch, P., and Brüstle, O. (2013). Leveling Waddington: the emergence of direct programming and the loss of cell fate hierarchies. Nat. Rev. Mol. Cell Biol. *14*, 225–236.

Lawson, K.A., Meneses, J.J., and Pedersen, R.A. (1991). Clonal analysis of epiblast fate during germ layer formation in the mouse embryo. Development *113*, 891–911.

Loh, K.M., and Lim, B. (2011). A precarious balance: pluripotency factors as lineage specifiers. Cell Stem Cell *8*, 363–369.

Loh, K.M., Ang, L.T., Zhang, J., Kumar, V., Ang, J., Auyeong, J.Q., Lee, K.L., Choo, S.H., Lim, C.Y., Nichane, M., et al. (2014). Efficient endoderm induction from human pluripotent stem cells by logically directing signals controlling lineage bifurcations. Cell Stem Cell *14*, 237–252.

Lohnes, D. (2003). The Cdx1 homeodomain protein: an integrator of posterior signaling in the mouse. BioEssays *25*, 971–980.

Mae, S., Shono, A., Shiota, F., Yasuno, T., Kajiwara, M., Gotoda-Nishimura, N., Arai, S., Sato-Otubo, A., Toyoda, T., Takahashi, K., et al. (2013). Monitoring and robust induction of nephrogenic intermediate mesoderm from human pluripotent stem cells. Nat. Commun. *4*, 1367.

Majesky, M.W. (2007). Developmental basis of vascular smooth muscle diversity. Arterioscler. Thromb. Vasc. Biol. *27*, 1248–1258.

Martin, B.L., and Kimelman, D. (2008). Regulation of canonical Wnt signaling by Brachyury is essential for posterior mesoderm formation. Dev. Cell *15*, 121–133.

Martin, B.L., and Kimelman, D. (2010). Brachyury establishes the embryonic mesodermal progenitor niche. Genes Dev. *24*, 2778–2783.

Marvin, M.J., Di Rocco, G., Gardiner, A., Bush, S.M., and Lassar, A.B. (2001). Inhibition of Wnt activity induces heart formation from posterior mesoderm. Genes Dev. *15*, 316–327.

McLean, A.B., D'Amour, K.A., Jones, K.L., Krishnamoorthy, M., Kulik, M.J., Reynolds, D.M., Sheppard, A.M., Liu, H., Xu, Y., Baetge, E.E., and Dalton, S. (2007). Activin a efficiently specifies definitive endoderm from human embryonic stem cells only when phosphatidylinositol 3-kinase signaling is suppressed. Stem Cells *25*, 29–38.

Merrill, B.J., Pasolli, H.A., Polak, L., Rendl, M., García-García, M.J., Anderson, K.V., and Fuchs, E. (2004). Tcf3: a transcriptional regulator of axis induction in the early embryo. Development *131*, 263–274.

Mummery, C.L., Ward, D., and Passier, R. (2007). Differentiation of human embryonic stem cells to cardiomyocytes by coculture with endoderm in serum-free medium. Curr. Protoc. Stem Cell Biol. *Chapter 1*, Unit 1F.2.

Murry, C.E., and Keller, G. (2008). Differentiation of embryonic stem cells to clinically relevant populations: lessons from embryonic development. Cell *132*, 661–680.

Niederreither, K., Vermot, J., Messaddeq, N., Schuhbaur, B., Chambon, P., and Dollé, P. (2001). Embryonic retinoic acid synthesis is essential for heart morphogenesis in the mouse. Development *128*, 1019–1031.

Nishikawa, S., Jakt, L.M., and Era, T. (2007). Embryonic stem-cell culture as a tool for developmental cell biology. Nat. Rev. Mol. Cell Biol. *8*, 502–507.

Nusse, R., and Varmus, H. (2012). Three decades of Wnts: a personal perspective on how a scientific field developed. EMBO J. *31*, 2670–2684.

Osorno, R., Tsakiridis, A., Wong, F., Cambray, N., Economou, C., Wilkie, R., Blin, G., Scotting, P.J., Chambers, I., and Wilson, V. (2012). The developmental dismantling of pluripotency is reversed by ectopic Oct4 expression. Development *139*, 2288–2298.

Savory, J.G.A., Pilon, N., Grainger, S., Sylvestre, J.-R., Béland, M., Houle, M., Oh, K., and Lohnes, D. (2009). Cdx1 and Cdx2 are functionally equivalent in vertebral patterning. Dev. Biol. *330*, 114–122.

Schultheiss, T.M., Xydas, S., and Lassar, A.B. (1995). Induction of avian cardiac myogenesis by anterior endoderm. Development *121*, 4203–4214.

Stern, C.D., Charité, J., Deschamps, J., Duboule, D., Durston, A.J., Kmita, M., Nicolas, J.-F., Palmeirim, I., Smith, J.C., and Wolpert, L. (2006). Head-tail patterning of the vertebrate embryo: one, two or many unresolved problems? Int. J. Dev. Biol. *50*, 3–15.

Tam, P.P., and Loebel, D.A. (2007). Gene function in mouse embryogenesis: get set for gastrulation. Nat. Rev. Genet. *8*, 368–381.

Tam, P.P., Parameswaran, M., Kinder, S.J., and Weinberger, R.P. (1997). The allocation of epiblast cells to the embryonic heart and other mesodermal lineages: the role of ingression and tissue movement during gastrulation. Development *124*, 1631–1642.

Tortelote, G.G., Manuel Hernández-Hernández, J., Quaresma, A.J., Nickerson, J.A., Imbalzano, A.N., and Rivera-Pérez, J.A. (2013). Wnt3 function in the epiblast is required for the maintenance but not the initiation of gastrulation in mice. Dev. Biol. *374*, 164–173.

Touboul, T., Hannan, N.R., Corbineau, S., Martinez, A., Martinet, C., Branchereau, S., Mainot, S., Strick-Marchand, H., Pedersen, R., Di Santo, J., et al. (2010). Generation of functional hepatocytes from human embryonic stem cells under chemically defined conditions that recapitulate liver development. Hepatology *51*, 1754–1765.

van Rooijen, C., Simmini, S., Bialecka, M., Neijts, R., van de Ven, C., Beck, F., and Deschamps, J. (2012). Evolutionarily conserved requirement of Cdx for post-occipital tissue emergence. Development *139*, 2576–2583.

Wu, C.I., Hoffman, J.A., Shy, B.R., Ford, E.M., Fuchs, E., Nguyen, H., and Merrill, B.J. (2012). Function of Wnt/β-catenin in counteracting Tcf3 repression through the Tcf3-β-catenin interaction. Development *139*, 2118–2129.

Xu, C., Tabebordbar, M., Iovino, S., Ciarlo, C., Liu, J., Castiglioni, A., Price, E., Liu, M., Barton, E.R., Kahn, C.R., et al. (2013). A zebrafish embryo culture system defines factors that promote vertebrate myogenesis across species. Cell *155*, 909–921.